Research Article

Double-epoch subtraction reveals long-latency mismatch response in urethane-anaesthetized mice

Jamie A. O'Reilly [a, b]

[a] College of Biomedical Engineering, Rangsit University, Pathumthani, Thailand.

[b] Department of Biomedical Engineering, University of Strathclyde, Glasgow, UK.

Present Address:

College of Biomedical Engineering, Rangsit University

52/347 Muang-Ake, Phaholyothin Road,

Pathum Thani 12000, Thailand

Phone: +66(0)64 783 4785

E-mail: jamie.o@rsu.ac.th

Abstract

Background Anaesthetized rodents are examined for their capacity to model human mismatch negativity (MMN). In the present study, oddball and deviant-alone control paradigms, with stimuli varying in frequency (ascending and descending) and intensity (louder and quieter), were presented to anaesthetized mice to determine whether they elicit a translational mismatch response (MMR).

New Method Resulting waveforms displayed long-latency (>200 ms post-stimulus) components, only made fully visible from oddball paradigm data by applying a double-epoch subtraction. In this approach, an extended epoch containing two consecutive standard evoked responses was subtracted from the response to an oddball followed by a standard (i.e. *oddball:standard* – *standard:standard*).

Results The trailing standard responses effectively cancelled each other out, revealing biphasic long-latency components. These MMR waveforms correlated strongly with deviant-alone paradigm evoked potentials >200 ms post-stimulus, potentially indicative of shared underlying mechanisms. Interestingly, these components were absent from the quieter oddball MMR.

Comparison with Existing Method(s) Classical mismatch negativity computation is incapable of fully characterizing the long-latency biphasic response observed from this study, due to the inbuilt constraint of a single stimulus epoch. These results also suggest that the deviant-alone paradigm may be considered akin to a positive control for sensory-memory disruption, widely thought to be at the root of MMN generation in humans.

Conclusions Long-latency auditory evoked potential components are observed from anaesthetized mice in response to frequency and increasing intensity oddball stimuli. These display some congruencies with human MMN.

Keywords Mismatch response; Mismatch negativity; Long-latency potentials; Oddball paradigm; Deviant-alone control

Declarations of interest None

1. Introduction

Mismatch negativity (MMN) is observed from humans presented with an auditory event which deviates from expected auditory input. This mismatch between expectation and actuality is referred to as a violation of sensory-memory, or prediction-error. Experimentally, this is typically invoked using some variant of the oddball (OD) paradigm, generally where a stable pattern of auditory stimulation (*standard*) is occasionally destabilized by infrequent, irregular changes in stimulation (*oddball/deviant*); MMN is classically derived from the difference between auditory evoked potential (AEP) induced by these two conditions. Conventionally, the standard AEP is subtracted from the oddball AEP. In humans, this typically manifests as negative peak amplitude between 100 and 250 ms post-stimulus-onset (Näätänen et al., 2012). This electrophysiological feature has garnered attention in clinical research, particularly for the examination of neuropsychiatric diseases; most noteworthy is that patients with schizophrenia repeatedly demonstrate lower amplitude MMN than healthy subjects (Erickson et al., 2016). This MMN response is widely thought to reflect deviance-detection, caused by a violation of sensory-memory or prediction error. This theory is not without contention, however, and several authors have offered alternative explanations, concentrating mainly on stimulus-specific adaptation (SSA), which is an observed phenomenon at multiple levels throughout the sensory nervous system (Klein et al., 2014; Nelken, 2014; Nelken and Ulanovsky, 2007), to explain MMN. In contrast, there has been a relative paucity of neurophysiological evidence, at the individual neuron level, for the proposed neural correlate of deviance-detection; although recent studies of prediction error have begun proving this mechanism (Näätänen et al., 2005; Parras et al., 2017). Use of the terminology, "stimulus-specific", may actually be an over-generalization, as current research does not thoroughly address adaptation caused by auditory features other than frequency, such as duration or intensity, which also elicit MMN (Todd et al., 2008). Ulanovsky et al. (2003) reported intensity-induced SSA in seven anaesthetized cats, as an adjunctive experiment that also found an absence of SSA to inter-stimulus-interval (ISI) variation; intriguingly, both intensity and ISI changes are considered capable of generating MMN (Näätänen et al., 2012). Another preliminary report demonstrated SSA to novel frequency, intensity, and interaural time difference stimuli, in four anaesthetized barn owls (Reches and Gutfreund, 2008). In contrast, a larger study in urethane-anaesthetized rats found SSA to frequency, but not intensity deviance (Duque et al., 2016). To the best of my knowledge, there is an absence of studies that convincingly demonstrate SSA to duration changes. On balance, the evidence of whether SSA is truly a general phenomenon that occurs in anaesthetized mice is inconclusive, and requires larger studies to provide more robust evidence. Perhaps frequency-specific adaptation would be a more fitting term, for the time being, lacking a substantial body of research into duration- and intensity-induced adaptation in auditory neurons. Thus, there remains some debate over the underlying neural source(s) and nature of mismatch negativity, and how exactly it is influenced in neuropsychiatric disease (Light and Näätänen, 2013; May and Tiitinen, 2010; Todd et al., 2012).

Rodents are one of the preferred model species for investigating MMN. After some initial negative and mixed results (Eriksson and Villa, 2005; Lazar and Metherate, 2003; Umbricht et al., 2005), anaesthetized rodents have largely been reported to demonstrate a *true* deviance-detection mismatch response (MMR), comparable with human MMN (Astikainen et al., 2011; Kurkela et al., 2018; Nakamura et al., 2011; Okazaki et al., 2006; Ruusuvirta et al., 2015, 2013, 1998; Tikhonravov et al., 2010, 2008). Anaesthetic agents and experimental procedures have varied considerably between studies (although urethane is the most commonly used anaesthetic), challenging direct comparisons of findings, which have also varied considerably. For instance, latency ranges of supposed rodent MMR peak amplitudes have extended from approximately 25 to 200 ms post-stimulus-onset, with both positive and negative polarities being reported. Although it has been

pointed out that latency and polarity are not necessarily qualifying factors for a *true* rodent MMR, given the vast neuroanatomical differences that exist between them and humans (Harms et al., 2016). The majority of this research has been in rats, and there are relatively few published studies using anaesthetized mice. There is an account of late mismatch responses, occurring approximately 200-400 ms post-stimulus-onset, recorded from excitatory and parvalbumin-positive neurons in the auditory cortex of anaesthetized mice; which the authors suggest might provide a link between SSA and MMN (Chen et al., 2015). Furthermore, mouse MMR studies almost exclusively focus on duration and frequency oddball paradigms. To the best of my knowledge, there are currently no published accounts of intensity oddball paradigms in anaesthetized mice.

The deviant-alone (DA) control is identical to the OD paradigm, except that standard stimuli are replaced with silence. Deviant/oddball stimuli are presented in precisely the same sequence, with silent gaps in between them. This form of control sequence emerged in the earliest published rodent MMR studies, with the intention of controlling for tone repetition rate (Eriksson and Villa, 2005; Lazar and Metherate, 2003; Ruusuvirta et al., 1998). Essentially, the DA condition was meant to dissociate any influence of SSA, or repetition-suppression, from the presence of a *true* sensory-memory disruption effect (Tikhonravov et al., 2008). Different presentation rates of standard and oddball stimuli in the OD paradigm cause an imbalance in adaptation between their corresponding target neural populations, which may manifest as evoked responses of unequal magnitude. When standard and oddball AEP waveforms are then subtracted, the resulting MMR simply reflects a decreased amplitude standard AEP relative to the oddball AEP, due to its higher presentation rate, hence greater level of adaptation, opposed to a separate deviance-detection component. This is the basis of the adaptation hypothesis of MMN. The initial theory supporting use of DA control paradigms is as follows: oddball stimuli are presented without any preceding standards, and are therefore considered to lack the proposed deviance-detection component that arises from a mismatch between expected and actual input; by comparing the AEP elicited by the same stimulus in OD and DA paradigms, it may be possible to identify whether the MMR truly reflects sensory-memory disruption, or a straightforward disparity of adaptation between standard and oddball responses caused by differential adaptation (Tikhonravov et al., 2008). However, this rationale has received criticism because the DA sequence inherently lengthens the inter-stimulus interval (ISI) and reduces the overall stimulation rate, both of which influence auditory activity (Nelken and Ulanovsky, 2007). Recent studies have tended towards other control paradigms that do not suffer from these drawbacks, such as the many-standards/equiprobable condition, which is considered by many to be a more appropriate control (Harms et al., 2014; Kurkela et al., 2018); although the DA paradigm does occasionally find use in contemporary studies (Polterovich et al., 2018).

In this study, the DA control paradigm is revisited, with an updated interpretation, as outlined in the Theory section. This is tested by applying a novel double-epoch subtraction to oddball paradigm waveforms, as described in the Calculation section, and comparing these difference waveforms with DA control waveforms. Fundamentally, this aims to further elucidate the MMR in urethane-anaesthetized mice; comparing both frequency and intensity MMR waveforms with corresponding DA paradigm evoked waveforms.

2. Material and methods

2.1 Animals

Fourteen laboratory mice (genetically >99.999% C57BL/6J) were used in this experiment. These were bred in-house at the University of Strathclyde's Biological Procedures Unit (BPU). This cohort consisted of nine males and five females, aged between 14 and 17 weeks ($\bar{x}$ = 15.4). Males weighed from 24.9 to 32.4 g ($\bar{x}$ = 27.8 g) and females weighed from 20.6 to 22.4 g ($\bar{x}$ = 24.4 g). No significant differences between sexes were observed from this study. Animal husbandry and housing practices followed standard United Kingdom Home Office guidelines, with mice housed in same-sex groups of two or more, inside an atmospherically controlled holding room at 21°C (±1°C), 55% relative humidity (±10%) with lights on from 0700 to 1900. Food and water were available *ad libitum*. All of these procedures were approved by the Animal Welfare and Ethical Review Body, University of Strathclyde, and performed in accordance with the United Kingdom Animals (Scientific Procedures) Act 1986.

2.2 Surgery

Three intraperitoneal injections of urethane, totalling 1.5g/kg, were staggered in twenty minute intervals to anesthetize mice; supplementary concentrations of 0.2g/kg were administered, as required, to achieve the desired state of unconsciousness. Anaesthetic depth was verified by ensuring absent tail-pinch, pedal, and corneal reflexes. When suitably anesthetized, animals were transferred into a stereotactic frame for rodents (Model 900; David Kopf Instruments, USA) and attached by their incisors to a mouse adapter (Model 923-B; David Kopf Instruments, USA). Their heads were clamped laterally with non-rupture zygomatic ear cups (Model 921; David Kopf Instruments, USA) to secure their skulls whilst avoiding damage to the auditory organs. They were placed on an isothermal heating pad (35°C) to support body temperature during surgery. Their head was shaved with an electric trimmer and hair removal cream (Nair; Church & Dwight Ltd., UK) was applied to remove any remaining fur. A scalp incision from rostral to caudal exposed the skull. The wound was held open by retracting the skin laterally using forceps to ensure an unobstructed working view of the skull. Membranous tissue above the skull was bluntly dissected before cleaning with 70 % ethanol and drying with compressed air (RS Components Ltd., UK). Cortical EEG electrode implantation sites were mapped out bilaterally above the primary auditory cortices (2.2 mm caudal and 3.8 mm lateral relative to Bregma) on the exposed skull using a stereotactic manipulator. These coordinates were obtained from a standardized C57 mouse brain atlas (Paxinos and Franklin, 2004). Shallow burr holes were drilled at these sites and 1 mm diameter skull-screw electrodes (Royem Scientific Ltd., UK) were slowly inserted, including a single reference placed centrally above the cerebellum, taking care not to penetrate the dura matter. These electrodes were oriented as previously described (O'Reilly, 2019a; Fig. 1). Wires wrapped around the electrodes (0.2 mm gauge) provided a conductive path between epidural field potentials and electronic amplification equipment. Following electrode implantation surgery, mice were immediately transferred into a recording chamber to begin the experiment.

2.3 Equipment

An acoustic startle cubicle (Med Associates Inc., USA) was customized with electromagnetic shielding and additional sound-absorbing foam (Paulstra Snc., France). This was fitted with an infrared digital

video camera in the ceiling, enabling a real-time view of the animal under test. Following surgery, mice were placed lying on top of an isothermal heating pad (35°C) inside of the recording chamber. A loudspeaker positioned facing the animal's head, at a distance of approximately 15 cm, was used to present auditory stimuli. This speaker was calibrated in sound pressure level (SPL) with a digital sound meter using the A-weighted scale (Model 33-2055; Radioshack, USA) placed at the approximate position of the animal's head. From inside the chamber, background acoustic noise levels measured below 55 dB. Electrode wires were connected to an amplifier board (RHD2132; Intan Technologies, USA) and epidural potentials were digitized at 1 kHz with on-board bandpass filtering between 0.1 and 500 Hz. Electrophysiology data and synchronization signals were viewed in real-time and stored for post hoc analyses using Open-Ephys GUI software (open-ephys.org). Auditory stimulation and synchronization pulses were generated in Matlab (Mathworks Inc., USA) and output via a USB data acquisition device (USB-6255; National Instruments, USA).

2.4 Auditory Paradigms

Balanced oddball (OD) paradigms consisting of both increasing and decreasing deviance oddballs were used in this study. These began with 20 consecutive standards, designed to support the formation of a stable sensory-memory trace. This was followed by either an increasing or decreasing oddball, or another standard, presented pseudo-randomly. Three consecutive standards were then presented, to ensure maintenance of the sensory-memory trace, followed by another standard or oddball interruption. This sequence was repeated for 1000 total presentations; 800 standards, 100 increasing oddballs, and 100 decreasing oddballs. Therefore, deviant stimuli accounted for 20 % of all oddball paradigm stimuli. Two OD paradigms were presented; one with oddball stimuli varying only in frequency, and one with stimuli varying only in intensity. In both frequency- and intensity-varying OD paradigms, standard stimuli were 100 ms, 10 kHz, 80 dB sinusoidal tones. Ascending and descending frequency oddball stimuli were 12.5 and 7.5 kHz, respectively, but otherwise their physical dimensions were identical to the standard. Similarly, louder and quieter oddball stimuli were 90 and 70 dB, respectively, but both were the same duration and frequency as the standard. A 450 ms offset-to-onset inter-stimulus interval (ISI) was applied, and auditory stimuli had instantaneous rise and fall times; this did not appear to cause any distortions to the epidural field potential. This design enabled an examination of both increases and decreases in individual physical features of the oddball paradigm. Each deviant-alone control paradigm was identical to the OD paradigm, but for one aspect: standard stimuli were silent. This effectively increased the ISI to at least 2100 ms, because of the three intervening standards rule. Both frequency- and intensity-varying DA control paradigms were presented. The order of paradigms was frequency OD, frequency DA, intensity OD, then intensity DA, with intervening silent periods lasting a couple of minutes. In total, these recordings lasted for approximately forty-five minutes.

2.5 Data Analysis

Auditory evoked potentials were computed with 100 ms pre-stimulus mean baseline correction. Animals were anaesthetized throughout the recordings, thus movement artefacts were negligible. A zero-phase-shift, digital bandpass filter was applied to further attenuate signals outside the range of 0.1 to 30 Hz. The AEP for each stimulus was conventionally produced by averaging, and grand-averages were the mean of all animals' respective AEP. To compute MMR difference waveforms, the method described in the Calculation section was applied. For the *standard-standard* AEP pair, the

first was two before the oddball, and the second was immediately preceding the oddball, as illustrated at the bottom of Figure 1b. The *oddball-standard* AEP pair consisted of the oddball and the consecutive standard. To facilitate a comparison of long-latency response morphology, without considering differences in magnitude, grand-average DA and MMR waveforms >200 ms were each normalized to values between −1 and 1. Normalized root-mean-squared error (NRMSE) was used to quantify the error, and the concordance correlation coefficient (CCC) was calculated to provide an index of the similarity between them (Lin, 2006). The NRMSE between normalized DA and MMR waveforms >200 ms post-stimulus-onset was measured for each animal. These were then compared with a one-way repeated-measures analysis of variance (rmANOVA) and follow-up pairwise comparisons with paired two-tailed T-tests. The threshold for rejecting the null hypothesis was set to 0.05 and Bonferroni corrections were applied to adjust the p-value for multiple comparisons. Furthermore, normalized waveforms were approximated by polynomial models to generalize their morphology. The degree of polynomial expression used to model each waveform was determined according to the criteria of achieving NRMSE < 5 %; although a limit of 30 was applied in any cases that failed to reach this criteria. Power spectral density (PSD) of DA and MMR grand-averages (>200 ms post-onset) across 0 to 30 Hz was calculated using Welch's method (Welch, 1967). This allowed an analysis of the frequency-domain signature of the observed long-latency potentials. To further quantify the observed biphasic long-latency response, mean-to-mean amplitude between 300 to 500 ms and 600 to 800 ms post-stimulus-onset measurement windows was recorded and analysed with rmANOVA and pairwise T-tests, as described above, with Bonferroni corrections for multiple comparisons. Where Mulchy's test of sphericity returned $p < 0.05$, the Greenhouse-Geisser method was used to adjust the degrees of freedom and corresponding p-value. This analysis was performed using Python 3, with third-party modules MNE (Gramfort et al., 2013), Scipy (Jones et al., 2001), and Scikit-Learn (Pedregosa et al., 2011). Statistical tests were performed using R Studio (R Team, 2018). The data described in this paper is available from an open-access repository (O'Reilly, 2019b).

3. Theory

This article offers an alternative interpretation of the deviant-alone control paradigm, providing some supporting data. Rather than simply controlling for stimulus presentation rate, which was initially proposed as its rationale (Ruusuvirta et al., 1998; Tikhonravov et al., 2008); conceptually, the DA condition might reasonably be considered as a form of positive control for sensory-memory violation. The oddball condition is hypothesized to activate independent sensory-memory-related neurophysiological processes, due to the disruption of a sensory-memory trace, which has more recently become known as a prediction-error (Parras et al., 2017); observed in the MMN or MMR component of the cortical AEP. It is strongly refuted that this might be a modification of obligatory sensory components due to adaptation, and the prevailing theory holds that the difference waveform reflects deviance-detection/sensory-memory disruption/prediction-error (Näätänen et al., 2005). In the predictive coding model of brain function, this is proposed to result from a continuous comparison between expected input, based on recent previous input, and actual input applied to the sensory-cognitive system (Wacongne et al., 2012). It therefore stands to reason, a stimulus presented against a background of relative silence (all standard stimuli are silent in DA paradigms) will more drastically deviate from previous and expected inputs than if recently preceded by a slightly different physical stimulus; thereby generating a corresponding MMN or MMR component. One downside of this interpretation is that there is no standard AEP with which to perform a waveform subtraction; making direct comparison with oddball paradigm difference waveforms challenging, and leaving this theory potentially untestable under certain conditions. There are also the aforementioned issues highlighted surrounding an effectively increased ISI and its effect on AEP amplitudes (Nelken and Ulanovsky, 2007). Nevertheless, long-latency potentials observed from this study appear to demonstrate a link between MMR and DA waveforms, illustrating the proposed function of the DA paradigm.

4. Calculation

Computation of the double-epoch difference waveform may be described most succinctly using an illustration (Figure 1). This presents the distinction between classical and double-epoch approaches to computing mismatch response waveforms from oddball paradigm data. In the classical method (Figure 1a), a single *standard* evoked response is subtracted from a single *oddball* evoked response, resulting in a MMR difference waveform which may present components occurring within the latency range of one full epoch; i.e. limited by the total onset-to-onset ISI. Components that might occur after this latency range, or extend beyond it, are beyond the reach of the conventional method. The double-epoch subtraction method (Figure 1b) was developed to overcome this limitation. In this approach, a pair of consecutive standard evoked responses is deducted from an oddball followed by a standard evoked response. The desired effect is that the two second standard evoked responses will cancel each other out, leaving the remaining waveform primarily influenced by the oddball. The double-epoch subtraction allows auditory evoked activity from the oddball to be observed beyond a single onset-to-onset window. In this study, this approach reveals long-latency potentials that otherwise would not be amenable to analyse.

5. Results

Grand-average AEP waveforms from frequency and intensity oddball paradigms are plotted in Figure 2. It can be seen that the double-epoch subtraction method has been applied. Stimulus on and off components are apparent in both epochs; these features occur <200 ms post-stimuli-onset. In each oddball-standard pair, there is a noticeable disparity between peak amplitudes of these early components; considered to arise due to different physical properties of the stimuli employed in their elicitation (Hillyard and Picton, 1978; Picton et al., 1977). This also causes alternate polarity deflections in MMR waveforms from decreasing versus increasing frequency or intensity deviance at ≈20 ms and ≈150 ms, associated with stimulus onset and offset responses, respectively. Interestingly, the MMR waveforms from both ascending and descending frequency oddballs, and louder intensity oddballs, appear to exhibit a long-latency positive potential, peaking between 300 and 500 ms, followed by a negative phase that peaks between 600 and 800 ms, before returning to baseline.

These double-epoch MMR waveforms are plotted alongside deviant-alone paradigm AEPs in Figure 3. The DA condition can be seen to elicit comparable waveform morphology, displaying a positive-to-negative biphasic response across the same temporal scale; although the peak amplitudes of these long-latency potentials are considerably greater than in MMR waveforms. This is consistent with the idea that the DA condition might act as an exaggerated oddball, producing a more pronounced sensory-memory disruption, or greater prediction-error.

To investigate the relationship between these MMR and DA responses, each was scaled to a dynamic range of −1 to 1; these normalized waveforms are plotted in Figure 4a-d. Fitted polynomials for each of these datasets are also displayed with dashed lines. The similarity between normalized MMR and DA waveforms was assessed with the concordance correlation coefficient (CCC), shown in Figure 4e-h. The CCC was 0.715, 0.916, and 0.929 for comparing 7.5 kHz, 12.5 kHz, and 90 dB MMR and DA waveforms, respectively, all indicating substantial similarity; these corresponded to normalized root-mean-squared error (NRMSE) measurements of 25.3, 14.0 and 12.1 %, respectively. In contrast, the 70 dB oddball MMR and DA waveforms had a CCC of −0.396 and NRMSE of 48.9 %, suggesting poor similarity. Details of polynomial expressions fitted to these normalized grand-averages provided in Table 1 demonstrate that DA waveforms can be modelled reasonably well (<5 % NRMSE) using less degrees (5 to 6) than MMR waveforms, which all required an 8 to 9 degree expression to reach the same level of accuracy; except for the 70 dB MMR, which could not be modelled with <5 % NRMSE using a polynomial function with less than 30 degrees.

These polynomial functions are plotted together in Figure 5a, illustrating similarity between all except from the quieter oddball MMR; this response may be generalized as the biphasic mean (i.e. the average without the normalized 70 dB MMR polynomial), which shows a positive deflection peaking at approximately 400 ms and a negative deflection peaking at approximately 700 ms. The power spectral density (PSD) of each grand-average MMR and DA waveform was analysed, and is displayed in Figure 5b. This suggests that the main frequency component of the observed long-latency biphasic response was between 2.5 and 5 Hz, given that this is comparably smaller in the 70 dB MMR than for the other waveforms, where a more pronounced peak is evident. The NRMSE from normalized DA and MMR waveforms >200 ms was also computed from each individual subject and graphed in Figure 5c. This data was compared with an rmANOVA, which produced a statistic of $F_{3,39}$ = 19.014 and p = 9.278 $\times 10^{-8}$. This exceeded the adjusted threshold for significance, thus the null hypothesis was rejected. Pairwise comparisons were performed to drill down on the source of this significant difference (Table 2), clearly identifying the culprit as the lower intensity oddball stimulus;

indicated on the histogram in Figure 5c. Mean-to-mean amplitude analysis also showed that the large biphasic response, going from positive to negative polarity across 300 to 500 ms and 600 to 800 ms latency windows, respectively, was comparably absent from quieter oddball-evoked MMR waveforms. This data is graphed in Figure 5d.

The rmANOVA performed on mean-to-mean amplitude data returned a statistically significant result ($F_{3.15,40.97}$ = 9.304, p = 6.443 $\times 10^{-5}$); the degrees of freedom and p-value were adjusted following failure of Mulchy's test. Pairwise comparisons reported in Table 3 indicate that the cause of this significant difference rests mainly with the lower intensity MMR, which was significantly smaller than DA waveforms, whereas other MMR mean-to-mean amplitudes were not significantly different from DA waveforms in one-to-one comparisons. This suggests that the biphasic response evoked by the DA condition is not elicited by quieter oddball stimuli. It was also found that overall, DA stimuli elicited greater amplitude biphasic responses than observed from MMR waveforms ($F_{1,13}$ = 34.376, p = 2 $\times 10^{-5}$; Bonferroni-adjusted), which reasserts the observations from Figure 2.

6. Discussion

In both frequency and intensity oddball paradigms, there is a visual disparity between stimulus onset and offset potential amplitudes of the first AEP, which were generated by physically distinct stimuli (Figure 2). These induce opposite polarity deflections for increasing and decreasing (frequency or intensity) oddballs in resulting MMR waveforms at the latencies of first AEP onset and offset response; i.e. peaking at approximately 20 and 125 ms, respectively. This is clearly caused by subtraction of a standard AEP with different onset and offset response amplitudes, which is unsurprising considering that both frequency and intensity have an influence over AEP amplitudes (Picton et al., 1977). In the second AEPs, which are both standards, onset and offset component amplitudes are not easily separable, because they are elicited by physically identical stimuli, and therefore do not cause such abrupt deflections in MMR trajectory at 570 or 675 ms (i.e. 20 or 125 ms post-second-stimulus-onset). This suggests that the two trailing standard stimuli do effectively cancel each other out to some degree, at least in terms of onset and offset potential amplitudes. The remaining MMR waveform from 200 to 1000 ms post-stimulus-onset consists of long-latency AEP components induced by the oddball condition. There is potentially concern over whether these waveform features also reflect physical sensitivities, which could be ascertained using the flip-flop control sequence (Harms et al., 2014); however, given that physical changes in opposite directions were applied in each oddball, resulting in shared general MMR latency-polarity trajectories >200 ms, the evidence suggests this is unlikely.

From comparing OD and DA paradigm waveforms in Figures 2 (OD AEPs and MMRs) and 3 (DA AEPs and OD MMRs), it should be recognized that onset and offset potentials evoked by the DA condition have greater amplitudes than those in OD paradigms, despite the stimuli being physically identical. This is caused by the inherently lengthened ISI in the DA paradigm, previously highlighted as one of its drawbacks (Nelken and Ulanovsky, 2007), as ISI generally has a proportional relationship with obligatory AEP amplitudes (Picton et al., 1977). Beyond onset and offset responses, >200 ms post-stimulus-onset, long-latency potentials emerge, which form a positive peak amplitude between 300 and 500 ms, followed by a negative polarity deflection peaking between 600 and 800 ms post-stimulus-onset. These may be characterized altogether as a long-latency biphasic response, although multiple underlying neural sources presumably contribute to the overall morphology of this waveform. Long-latency AEP components are thought to reflect higher-order processing, potentially involving bi-directional communication and integration of signals at different levels of the auditory system (Pratt et al., 2011). The biphasic response observed here was not significantly influenced by the frequencies or intensities employed (Figure 5d), in agreement with previous findings of long-latency potentials in mice (Ehlers and Somes, 2002). It is beyond the accepted latency range for human MMN (100-250 ms; Näätänen et al., 2012); hence uncertain how it relates to this component. These waveforms are also unlikely to be directly related to the human P3b response that occurs during directed attention towards a salient event, given that animals in this study were anesthetized. However, the human P3a response occurs at a similar latency range and can be evoked by frequency-deviant stimuli while subjects are unconscious (Koelsch et al., 2006; Plourde et al., 1993; Tavakoli et al., 2019). In a nonhuman primate model, P3a amplitude has been shown to diminish following ketamine administration, indicating that this component relies partially on intact NMDA receptor function, congruent with findings from humans (Gil-da-Costa et al., 2013). It may be tentatively posited that long-latency potentials observed in the present study are a rodent analogue of the human P3a response; representing late deviance-detection of primary auditory cortex neurons, previously recorded from anaesthetised mice (Chen et al., 2015). Functionally, these long-latency potentials may signify activation of the hierarchical prediction error circuit, described by Parras et al.

(2017), that may also incorporate connectivity with the hippocampus, which is widely implicated in the sensory-memory aspect of mismatch negativity (Ruusuvirta et al., 2015, 2013).

In the seminal work by Ruusuvirta et al. (1998), urethane-anaesthetized rats exhibited a slow positive amplitude deflection in the DA control AEP, which peaked at approximately 300 ms post stimulus. This was reported to deviate from frequency oddball paradigm AEPs after approximately 200 ms post-stimulus-onset. This may feasibly reflect the positive half-cycle of the biphasic response observed from the DA condition in the present study. However, the authors do not address the DA waveform sufficiently in their discussion, perhaps because the oddball paradigm did not evoke a similar response. Furthermore, waveforms are only plotted up to 350 ms post stimuli onset; limited by a single onset-to-onset ISI. One possible reason why this long-latency feature was not observed from oddball stimuli may be the closeness of frequencies employed as standards and oddballs (500 Hz separation) relative to the present study (2.5 kHz separation). Interestingly, there appears not to have been any follow-up investigation of these long-latency potentials evoked by the DA paradigm. Other evidence also suggests that positive long-latency potentials, peaking within the 200 to 400 ms post-stimulus latency window, may be elicited from mice and vary by genotype (Ehlers and Somes, 2002). In the present study, DA paradigm waveforms were analysed across a long epoch (up to 1000 ms post-stimulus), which revealed that the completion of this response, in addition to the positive peak described in previous studies, consists of a negative under-shoot before returning to baseline. Development of a novel double-stimulus AEP subtraction method enabled a comparison between these DA-evoked long-latency potentials with the oddball-evoked long-latency MMR. Previous studies may have facilitated an examination of long-latency potentials by incorporating a longer period between stimuli (Horváth et al., 2008; Javitt et al., 1998); although, lengthening ISI is reported to decrease MMN amplitude (Javitt et al., 1998; Michie et al., 2000), restricting the scope of this approach. In comparison, the proposed double-epoch subtraction does not require a lengthened ISI, and may be applied retroactively to electrophysiology data acquired during similar oddball paradigms.

Prominent contrasts to note while inspecting DA and MMR waveforms in Figure 3 are that onset and offset potentials present in DA paradigm AEPs appear to be extinguished by 200 ms, and that long-latency potential amplitudes are greater in response to DA paradigm stimuli. In terms of similarities, long-latency MMRs generated by frequency and increasing intensity oddball stimuli display comparable (although relatively diminutive) waveform morphology, consisting of positive and negative half-cycles, which peak at similar latencies to DA waveform long-latency potentials. This lends support for interpreting the DA condition as an exaggerated oddball; i.e. a stimulus presented within a recent context of silence will cause a more pronounced sensory-memory disruption, or prediction-error, than if recently preceded by a slightly different auditory stimulus. From this perspective, a repetitive standard stimulus is not necessarily required to prime the underlying pre-attentive neurosensory mechanisms; auditory sensory-memory, or predictions, are formed by the dynamic context of an organism's environment, and any disruption of relative stability, whether consisting of quietness or repetitive background stimulation, will cause an MMR, or prediction-error, corresponding to the degree of difference, which is an accepted property of MMN (Näätänen, 2018). Although lacking a standard stimulus removes the possibility of applying the AEP subtraction most associated with MMN. When normalized MMR and DA waveforms are plotted alongside one another in Figure 4, these similarities in morphology are apparent; potentially suggestive of common underlying neural generators. There may be an argument to say that the negative half-cycle is induced by the second standard stimulus; speculatively related to stimulus-switching or sensory-gating effects (Boutros and Belger, 1999). The second standard may even act as a kind of compounded oddball. Certainly, without a control paradigm omitting the following standard, it would be near-impossible to exclude these as potential sources of the negative-going half-cycle of the

biphasic response. However, DA paradigm stimuli, which were not immediately followed by another stimulus, also produce a transition from positive to negative polarity at comparable latencies (e.g. Figure 5a). Furthermore, analysis of NRMSE between normalized MMR and DA waveforms >200 ms indicates that frequency and increasing intensity oddballs evoke a long-latency MMR with reasonably similar morphology to corresponding DA paradigm waveforms; in contrast with quieter oddball stimuli, which displayed significantly greater error between normalized MMR and DA waveforms. Mean-to-mean amplitude data also illustrates this point; quieter oddball MMR waveforms do not present the same positive-to-negative response between 300 to 500 ms and 600 to 800 ms post-stimulus-onset. Moreover, by inspection, peak power at 2.5 to 5 Hz from the lower intensity MMR is negligible when compared with other MMR and DA waveform PSD plots. Taken together, this data suggests that the quieter deviant condition does not elicit the same long-latency components as frequency and increasing intensity oddballs in urethane-anaesthetized mice.

The finding that comparable long-latency potentials were absent from the lower intensity oddball response may offer direction for conceptualizing their psycho-physiological significance. Mismatch negativity is thought to arise from any discriminable change in stimulus properties (Pakarinen et al., 2007), although these MMR waveforms appear to be caused by *environmentally salient* changes in auditory input; based on the deduction that quieter stimuli are less salient than increasing intensity or different frequency stimuli relative to a constant standard, thus why they do not evoke the same long-latency potentials. Henceforth, it may be tentatively suggested that these long-latency biphasic responses reflect something more akin to an upstream neural correlate of the acoustic orienting response (Barham and Boersma, 1975). Crucially, there is a lack of research using intensity oddball paradigms with increasing and decreasing deviants, therefore this must remain an open question until it can be established whether, under any different contexts, a decrement in SPL can indeed elicit a *true* MMR in mice. Although some articles have reported human MMN responses to lower intensity oddball stimuli, these typically include a low number of subjects (Näätänen et al., 1989; Pakarinen et al., 2007). It can also be challenging to interpret results when only difference waveforms are shown, without the underlying standard and oddball AEPs (Lee et al., 2017). Moreover, the predominance of MMN literature relates to frequency and duration changes (Näätänen et al., 2012); with studies of intensity deviance tending to concentrate on louder oddball stimuli (e.g. Todd et al., 2008). It may also be worth reiterating that much of the literature citing *stimulus-specific* adaptation almost exclusively deals with frequency. There is currently no strong evidence, as I am aware, to suggest that the same adaptive processes occur in response to other physical properties of auditory stimuli, such as duration or intensity; an examination in mice actually suggests otherwise (Duque et al., 2016). The present study provides evidence to indicate that quieter oddball stimuli do not cause an MMR comparable with either frequency or increasing intensity stimuli in anaesthetized mice; raising the question of whether this reflects true change detection, or if more subtlety is involved in the generation of difference waveforms caused by manipulating different physical properties.

In summary, by applying a double-epoch subtraction between *oddball-standard* and *standard-standard* AEP pairs (Figure 1 and Figure 2), a series of biphasic long-latency potentials were observed from ascending and descending frequency, and louder intensity oddball stimuli. These display some properties in keeping with the deviance-detection hypothesis of MMN, and may reflect the same underlying mechanisms as previous long-latency AEPs recorded from rodents in oddball and deviant-alone conditions (Chen et al., 2015; Ehlers and Somes, 2002; Ruusuvirta et al., 1998), potentially related to the human P3a component (Koelsch et al., 2006; Plourde et al., 1993; Tavakoli et al., 2019). Interestingly, decreasing intensity oddballs did not elicit the same response, adding further nuance to the discussion in terms of whether *indiscriminate* versus *environmentally-salient* deviance-detection may be responsible for generating mismatch responses in rodents.

7. Acknowledgments

I gratefully acknowledge the doctoral supervision of Professors Bernard A. Conway and Judith A. Pratt, and Strathclyde Institute for Pharmacy and Biomedical Sciences for the provision of resources. This research was supported in part by the United Kingdom Engineering and Physical Sciences Research Council (grant no. EP/L015595/1).

8. References

Astikainen, P., Stefanics, G., Nokia, M., Lipponen, A., Cong, F., Penttonen, M., Ruusuvirta, T., 2011. Memory-Based Mismatch Response to Frequency Changes in Rats. PLoS One 6, e24208. https://doi.org/10.1371/journal.pone.0024208

Barham, R.M., Boersma, F.J., 1975. Orienting responses in a selection of cognitive tasks. Rotterdam University Press.

Boutros, N.N., Belger, A., 1999. Midlatency evoked potentials attenuation and augmentation reflect different aspects of sensory gating. Biol. Psychiatry 45, 917–922. https://doi.org/10.1016/S0006-3223(98)00253-4

Chen, I.-W., Helmchen, F., Lütcke, H., 2015. Specific Early and Late Oddball-Evoked Responses in Excitatory and Inhibitory Neurons of Mouse Auditory Cortex. J. Neurosci. 35, 12560–73. https://doi.org/10.1523/JNEUROSCI.2240-15.2015

Duque, D., Wang, X., Nieto-Diego, J., Krumbholz, K., Malmierca, M.S., 2016. Neurons in the inferior colliculus of the rat show stimulus-specific adaptation for frequency, but not for intensity. Sci. Rep. 6. https://doi.org/10.1038/srep24114

Ehlers, C.L., Somes, C., 2002. Long latency event-related potentials in mice: effects of stimulus characteristics and strain. Brain Res. 957, 117–128. https://doi.org/10.1016/S0006-8993(02)03612-0

Erickson, M.A., Ruffle, A., Gold, J.M., 2016. A Meta-Analysis of Mismatch Negativity in Schizophrenia: From Clinical Risk to Disease Specificity and Progression. Biol. Psychiatry 79, 980–987. https://doi.org/10.1016/J.BIOPSYCH.2015.08.025

Eriksson, J., Villa, A.E.P., 2005. Event-related potentials in an auditory oddball situation in the rat, in: BioSystems. pp. 207–212. https://doi.org/10.1016/j.biosystems.2004.09.017

Gil-da-Costa, R., Stoner, G.R., Fung, R., Albright, T.D., 2013. Nonhuman primate model of schizophrenia using a noninvasive EEG method. Proc. Natl. Acad. Sci. U. S. A. 110, 15425–30. https://doi.org/10.1073/pnas.1312264110

Gramfort, A., Luessi, M., Larson, E., Engemann, D.A., Strohmeier, D., Brodbeck, C., Goj, R., Jas, M., Brooks, T., Parkkonen, L., others, 2013. MEG and EEG data analysis with MNE-Python. Front. Neurosci. 7, 267.

Harms, L., Fulham, W.R., Todd, J., Budd, T.W., Hunter, M., Meehan, C., Penttonen, M., Schall, U., Zavitsanou, K., Hodgson, D.M., Michie, P.T., 2014. Mismatch negativity (MMN) in freely-moving rats with several experimental controls. PLoS One 9. https://doi.org/10.1371/journal.pone.0110892

Harms, L., Michie, P.T., Näätänen, R., 2016. Criteria for determining whether mismatch responses

exist in animal models: Focus on rodents. Biol. Psychol. https://doi.org/10.1016/j.biopsycho.2015.07.006

Hillyard, S.A., Picton, T.W., 1978. On and off components in the auditory evoked potential. Percept. Psychophys. 24, 391–398.

Horváth, J., Winkler, I., Bendixen, A., 2008. Do N1/MMN, P3a, and RON form a strongly coupled chain reflecting the three stages of auditory distraction? Biol. Psychol. 79, 139–147. https://doi.org/10.1016/j.biopsycho.2008.04.001

Javitt, D.C., Grochowski, S., Shelley, A.M., Ritter, W., 1998. Impaired mismatch negativity (MMN) generation in schizophrenia as a function of stimulus deviance, probability, and interstimulus/interdeviant interval. Electroencephalogr. Clin. Neurophysiol. 108, 143–53.

Jones, E., Oliphant, T., Peterson, P., 2001. SciPy: Open source scientific tools for Python.

Klein, C., Von Der Behrens, W., Gaese, B.H., 2014. Stimulus-specific adaptation in field potentials and neuronal responses to frequency-modulated tones in the primary auditory cortex. Brain Topogr. 27, 599–610. https://doi.org/10.1007/s10548-014-0376-4

Koelsch, S., Heinke, W., Sammler, D., Olthoff, D., 2006. Auditory processing during deep propofol sedation and recovery from unconsciousness. Clin. Neurophysiol. 117, 1746–1759. https://doi.org/10.1016/j.clinph.2006.05.009

Kurkela, J.L.O., Lipponen, A., Kyläheiko, I., Astikainen, P., 2018. Electrophysiological evidence of memory-based detection of auditory regularity violations in anesthetized mice. Sci. Rep. 8, 3027. https://doi.org/10.1038/s41598-018-21411-z

Lazar, R., Metherate, R., 2003. Spectral interactions, but no mismatch negativity, in auditory cortex of anesthetized rat. Hear. Res. 181, 51–56. https://doi.org/10.1016/S0378-5955(03)00166-7

Lee, M., Sehatpour, P., Hoptman, M.J., Lakatos, P., Dias, E.C., Kantrowitz, J.T., Martinez, A.M., Javitt, D.C., 2017. Neural mechanisms of mismatch negativity dysfunction in schizophrenia. Mol. Psychiatry 22. https://doi.org/10.1038/mp.2017.3

Light, G.A., Näätänen, R., 2013. Mismatch negativity is a breakthrough biomarker for understanding and treating psychotic disorders. Proc. Natl. Acad. Sci. 110, 15175–15176.

Lin, L.I.-K., 2006. A Concordance Correlation Coefficient to Evaluate Reproducibility. Biometrics 45, 255. https://doi.org/10.2307/2532051

May, P.J.C., Tiitinen, H., 2010. Mismatch negativity (MMN), the deviance-elicited auditory deflection, explained. Psychophysiology. https://doi.org/10.1111/j.1469-8986.2009.00856.x

Michie, P.T., Budd, T.W., Todd, J., Rock, D., Wichmann, H., Box, J., Jablensky, A. V, 2000. Duration and frequency mismatch negativity in schizophrenia. Clin. Neurophysiol. 111, 1054–1065. https://doi.org/10.1016/S1388-2457(00)00275-3

Näätänen, R., 2018. Attention and Brain Function, Attention and Brain Function. https://doi.org/10.4324/9780429487354

Näätänen, R., Jacobsen, T., Winkler, I., 2005. Memory-based or afferent processes in mismatch negativity (MMN): A review of the evidence. Psychophysiology. https://doi.org/10.1111/j.1469-8986.2005.00256.x

Näätänen, R., Kujala, T., Escera, C., Baldeweg, T., Kreegipuu, K., Carlson, S., Ponton, C., 2012. The mismatch negativity (MMN)--a unique window to disturbed central auditory processing in ageing and different clinical conditions. Clin. Neurophysiol. 123, 424–458.

Näätänen, R., Paavilainen, P., Alho, K., Reinikainen, K., Sams, M., 1989. Do event-related potentials reveal the mechanism of the auditory sensory memory in the human brain? Neurosci. Lett. 98, 217–221. https://doi.org/10.1016/0304-3940(89)90513-2

Nakamura, T., Michie, P.T., Fulham, W.R., Todd, J., Budd, T.W., Schall, U., Hunter, M., Hodgson, D.M., 2011. Epidural auditory event-related potentials in the rat to frequency and duration deviants: evidence of mismatch negativity? Front. Psychol. 2, 367.

Nelken, I., 2014. Stimulus-specific adaptation and deviance detection in the auditory system: experiments and models. Biol. Cybern. https://doi.org/10.1007/s00422-014-0585-7

Nelken, I., Ulanovsky, N., 2007. Mismatch Negativity and Stimulus-Specific Adaptation in Animal Models. J. Psychophysiol. 21, 214–223. https://doi.org/10.1027/0269-8803.21.34.214

O'Reilly, J.A., 2019a. Event-related potential arithmetic to analyze offset potentials from conscious mice. J. Neurosci. Methods 318, 78–83. https://doi.org/10.1016/j.jneumeth.2019.01.018

O'Reilly, J.A., 2019b. Frequency and intensity oddball and deviant-alone control paradigms in urethane-anesthetized mice. Mendeley Data 1. https://doi.org/10.17632/NDWHY5DRM5.1

Okazaki, S., Kanoh, S., Takaura, K., Tsukada, M., Oka, K., 2006. Change detection and difference detection of tone duration discrimination. Neuroreport 17, 395–399. https://doi.org/10.1097/01.wnr.0000204979.91253.7a

Pakarinen, S., Takegata, R., Rinne, T., Huotilainen, M., Näätänen, R., 2007. Measurement of extensive auditory discrimination profiles using the mismatch negativity (MMN) of the auditory event-related potential (ERP). Clin. Neurophysiol. 118, 177–185.

Parras, G.G., Nieto-Diego, J., Carbajal, G. V., Valdés-Baizabal, C., Escera, C., Malmierca, M.S., 2017. Neurons along the auditory pathway exhibit a hierarchical organization of prediction error. Nat. Commun. 8, 2148. https://doi.org/10.1038/s41467-017-02038-6

Paxinos, G., Franklin, K.B.J., 2004. The mouse brain in stereotaxic coordinates.

Pedregosa, F., Varoquaux, G., Gramfort, A., Michel, V., Thirion, B., Grisel, O., Blondel, M., Prettenhofer, P., Weiss, R., Dubourg, V., Vanderplas, J., Passos, A., Cournapeau, D., Brucher, M., Perrot, M., Duchesnay, É., 2011. Scikit-learn: Machine Learning in Python. J. Mach. Learn. Res. https://doi.org/10.1007/s13398-014-0173-7.2

Picton, T.W., Woods, D.L., Baribeau-Braun, J., Healey, T.M.G., 1977. Evoked potential audiometry. J Otolaryngol 6, 90–119.

Plourde, G., Joffe, D., Villemure, C., Trahan, M., 1993. The P3a Wave of the Auditory Event-related Potential Reveals Registration of Pitch Change during Sufentanil Anesthesia for Cardiac Surgery. Anesthesiol. J. Am. Soc. Anesthesiol. 78, 498–509.

Polterovich, A., Jankowski, M.M., Nelken, I., 2018. Deviance sensitivity in the auditory cortex of freely moving rats. PLoS One 13, e0197678. https://doi.org/10.1371/journal.pone.0197678

Pratt, H., Luck, S.J., Kappenman, E.S., 2011. The Oxford handbook of event-related potential components, The Oxford handbook of event-related potential components. Oxford university press.

Reches, A., Gutfreund, Y., 2008. Stimulus-Specific Adaptations in the Gaze Control System of the Barn Owl. J. Neurosci. 28, 1523–1533. https://doi.org/10.1523/jneurosci.3785-07.2008

Ruusuvirta, T., Lipponen, A., Pellinen, E., Penttonen, M., Astikainen, P., 2013. Auditory Cortical and Hippocampal-System Mismatch Responses to Duration Deviants in Urethane-Anesthetized

Rats. PLoS One 8, e54624. https://doi.org/10.1371/journal.pone.0054624

Ruusuvirta, T., Lipponen, A., Pellinen, E.K., Penttonen, M., Astikainen, P., 2015. Auditory cortical and hippocampal local-field potentials to frequency deviant tones in urethane-anesthetized rats: An unexpected role of the sound frequencies themselves. Int. J. Psychophysiol. 96, 134–140. https://doi.org/10.1016/j.ijpsycho.2015.04.007

Ruusuvirta, T., Penttonen, M., Korhonen, T., 1998. Auditory cortical event-related potentials to pitch deviances in rats. Neurosci. Lett. 248, 45–48.

Tavakoli, P., Dale, A., Boafo, A., Campbell, K., 2019. Evidence of P3a During Sleep, a Process Associated With Intrusions Into Consciousness in the Waking State. Front. Neurosci. 12, 1028. https://doi.org/10.3389/fnins.2018.01028

Team, R.C., 2018. R: A Language and Environment for Statistical Computing.

Tikhonravov, D., Neuvonen, T., Pertovaara, A., Savioja, K., Ruusuvirta, T., Näätänen, R., Carlson, S., 2010. Dose-related effects of memantine on a mismatch negativity-like response in anesthetized rats. Neuroscience 167, 1175–1182. https://doi.org/10.1016/J.NEUROSCIENCE.2010.03.014

Tikhonravov, D., Neuvonen, T., Pertovaara, A., Savioja, K., Ruusuvirta, T., Näätänen, R., Carlson, S., 2008. Effects of an NMDA-receptor antagonist MK-801 on an MMN-like response recorded in anesthetized rats. Brain Res. 1203, 97–102. https://doi.org/10.1016/J.BRAINRES.2008.02.006

Todd, J., Michie, P.T., Schall, U., Karayanidis, F., Yabe, H., Näätänen, R., 2008. Deviant Matters: Duration, Frequency, and Intensity Deviants Reveal Different Patterns of Mismatch Negativity Reduction in Early and Late Schizophrenia. Biol. Psychiatry 63, 58–64. https://doi.org/10.1016/J.BIOPSYCH.2007.02.016

Todd, J., Michie, P.T., Schall, U., Ward, P.B., Catts, S. V., 2012. Mismatch negativity (MMN) reduction in schizophrenia-Impaired prediction-error generation, estimation or salience? Int. J. Psychophysiol. https://doi.org/10.1016/j.ijpsycho.2011.10.003

Ulanovsky, N., Las, L., Nelken, I., 2003. Processing of low-probability sounds by cortical neurons. Nat. Neurosci. 6, 391–398. https://doi.org/10.1038/nn1032

Umbricht, D., Vyssotki, D., Latanov, A., Nitsch, R., Lipp, H.P., 2005. Deviance-related electrophysiological activity in mice: Is there mismatch negativity in mice? Clin. Neurophysiol. 116, 353–363. https://doi.org/10.1016/j.clinph.2004.08.015

Wacongne, C., Changeux, J.-P., Dehaene, S., 2012. A Neuronal Model of Predictive Coding Accounting for the Mismatch Negativity. J. Neurosci. 32, 3665–3678. https://doi.org/10.1523/JNEUROSCI.5003-11.2012

Welch, P.D., 1967. The use of fast Fourier transform for the estimation of power spectra: a method based on time averaging over short, modified periodograms. IEEE Trans. Audio Electroacoust 15, 70–73.

9. Tables

Table 1 Degree and error of polynomial models fit to grand-average mismatch response and deviant-alone waveforms.

Waveform	Degree	NRMSE
7.5 kHz MMR	9	4.0 %
7.5 kHz DA	5	4.2 %
12.5 kHz MMR	8	4.8 %
12.5 kHz DA	6	4.5 %
70 dB MMR	30	5.5 %
70 dB DA	6	3.6 %
90 dB MMR	8	4.3 %
90 dB DA	6	4.9 %

Table 2 Pairwise comparisons of normalized root-mean-squared error between normalized mismatch response and deviant-alone waveforms.

	12.5 kHz NRMSE	*7.5 kHz NRMSE*	*90 dB NRMSE*
7.5 kHz NRMSE	1.00	-	-
90 dB NRMSE	1.00	0.94	-
70 dB NRMSE	**2.5×10^{-6}**	**4.7×10^{-5}**	**2.7×10^{-7}**

Bonferroni-adjusted p-values; significant differences are highlighted in bold.

Table 3 Pairwise comparisons of mean-to-mean amplitude measurements from mismatch response and deviant-alone waveforms.

	7.5 kHz MMR	*7.5 kHz DA*	*12.5 kHz MMR*	*12.5 kHz DA*	*70 dB MMR*	*70 dB DA*	*90 dB MMR*
7.5 kHz DA	1.00	-	-	-	-	-	-
12.5 kHz MMR	1.00	0.320	-	-	-	-	-
12.5 kHz DA	0.705	1.00	0.367	-	-	-	-
70 dB MMR	0.729	**3.6×10^{-4}**	1.00	**4.4×10^{-4}**	-	-	-
70 dB DA	1.00	1.00	1.00	1.00	**0.050**	-	-
90 dB MMR	1.00	0.810	1.00	0.914	0.558	1.00	-
90 dB DA	1.00	1.00	1.00	1.00	**0.025**	1.00	1.00

Bonferroni-adjusted p-values; significant differences are highlighted in bold.

10. Figures

Figure 1:

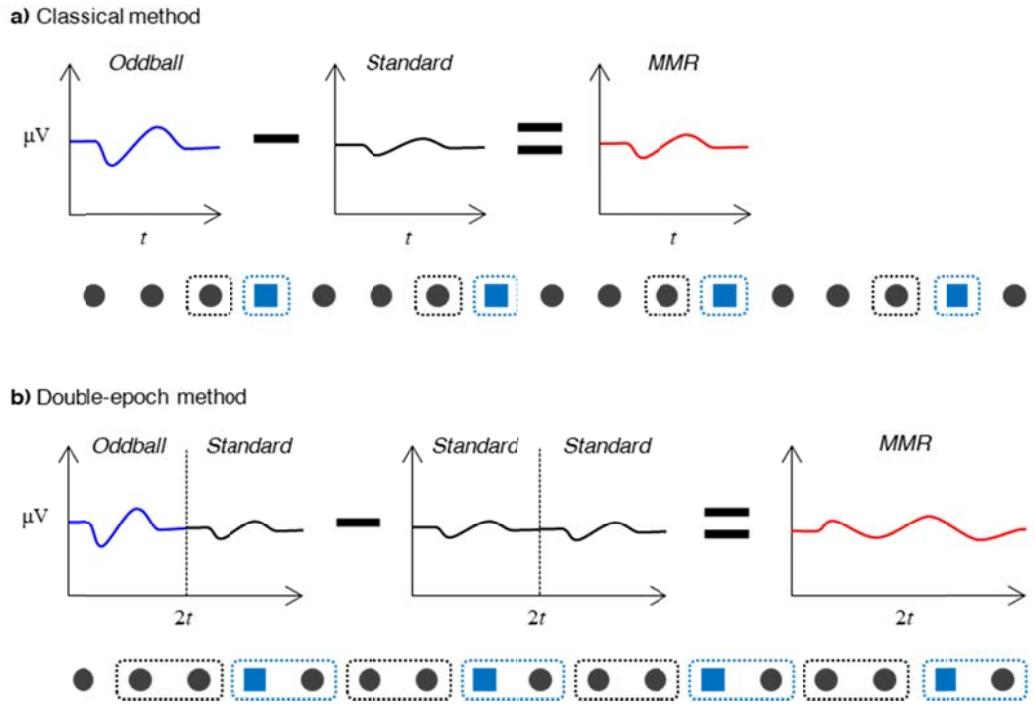

Figure 2:

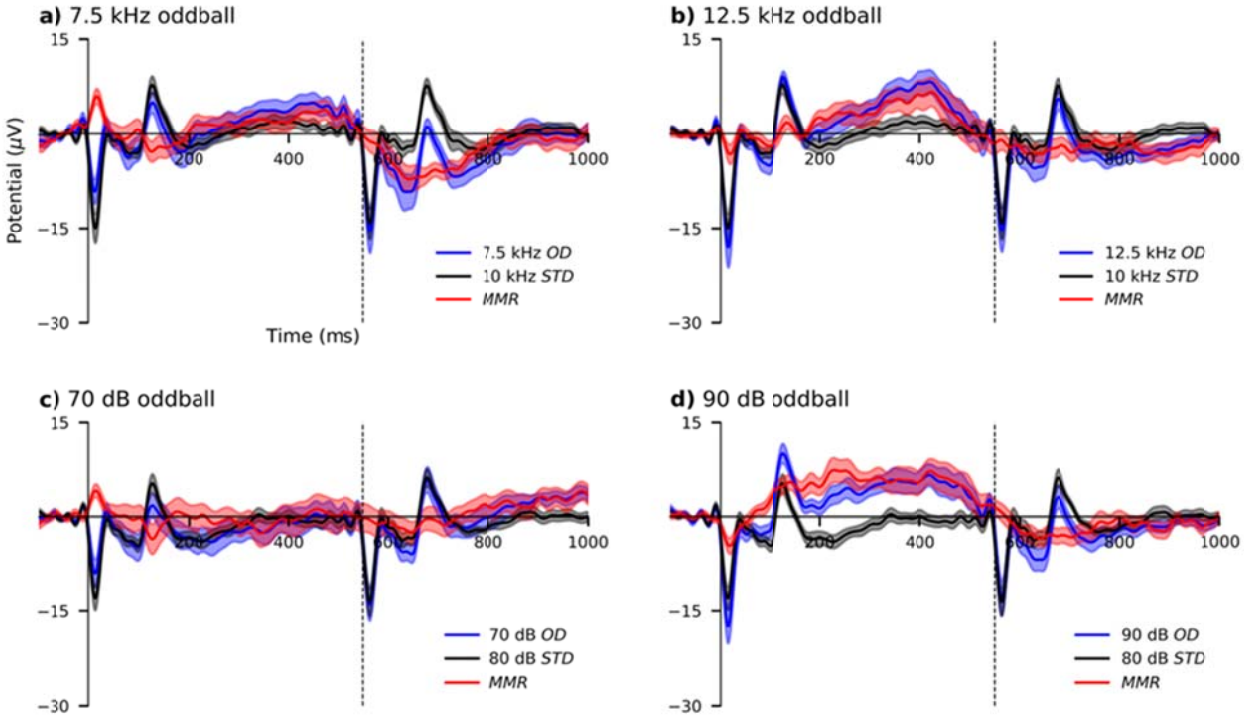

Figure 3:

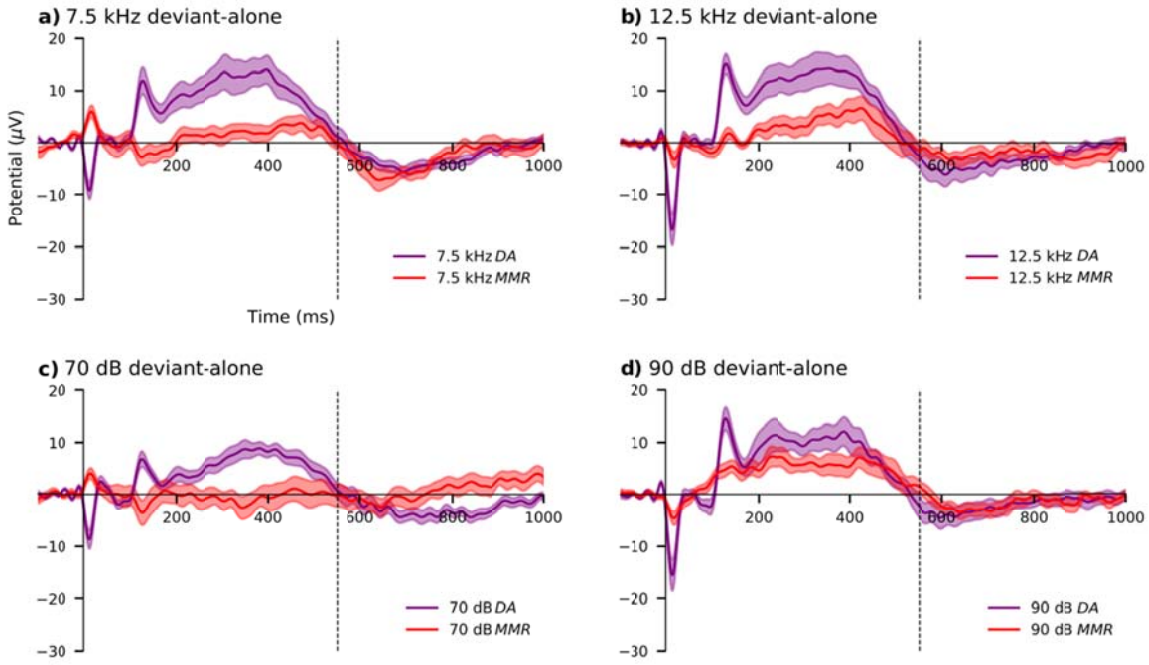
a) 7.5 kHz deviant-alone
b) 12.5 kHz deviant-alone
c) 70 dB deviant-alone
d) 90 dB deviant-alone
Potential (μV)
Time (ms)
7.5 kHz DA
7.5 kHz MMR
12.5 kHz DA
12.5 kHz MMR
70 dB DA
70 dB MMR
90 dB DA
90 dB MMR

Figure 4:

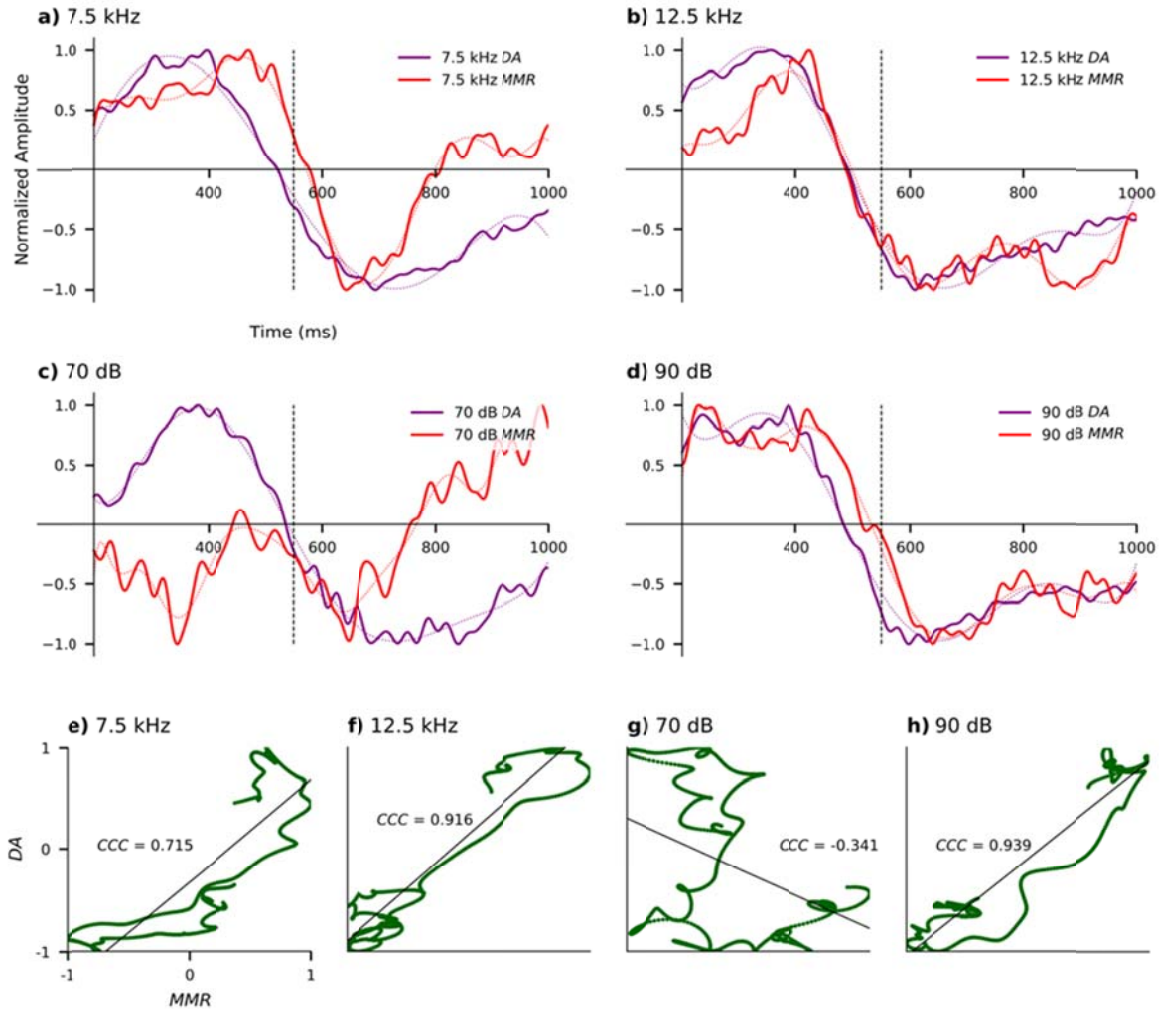
a) 7.5 kHz
b) 12.5 kHz
c) 70 dB
d) 90 dB
7.5 kHz DA
7.5 kHz MMR
12.5 kHz DA
12.5 kHz MMR
70 dB DA
70 dB MMR
90 dB DA
90 dB MMR
Normalized Amplitude
Time (ms)
e) 7.5 kHz
f) 12.5 kHz
g) 70 dB
h) 90 dB
CCC = 0.715
CCC = 0.916
CCC = -0.341
CCC = 0.939
DA
MMR

Figure 5:

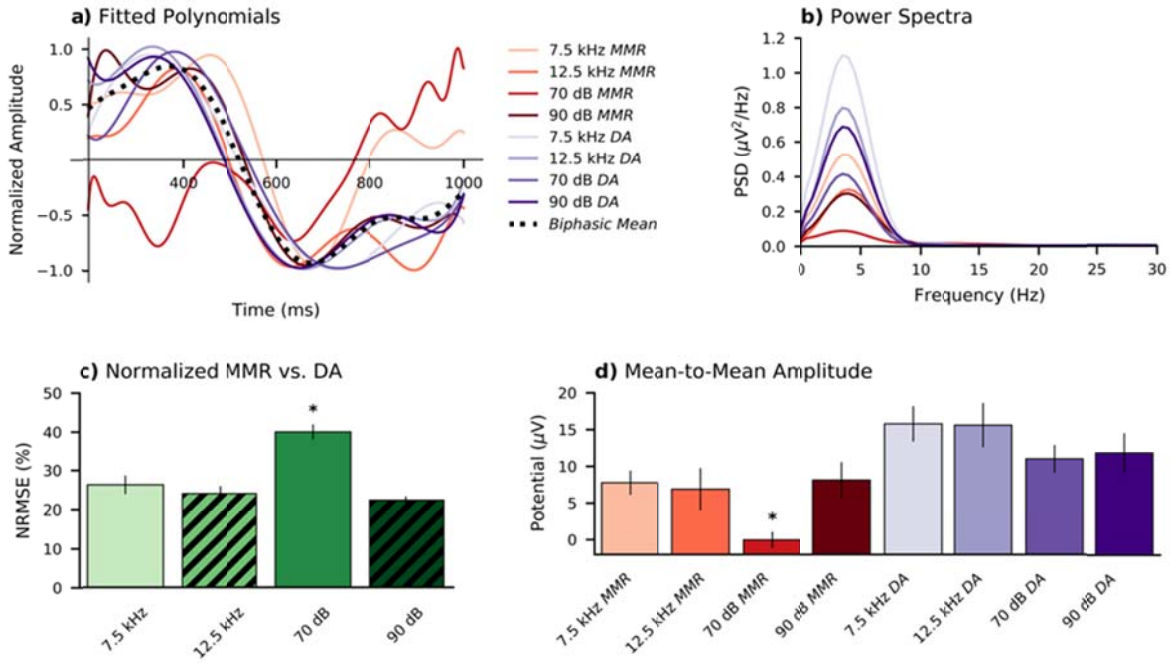
a) Fitted Polynomials
Normalized Amplitude
Time (ms)
7.5 kHz MMR
12.5 kHz MMR
70 dB MMR
90 dB MMR
7.5 kHz DA
12.5 kHz DA
70 dB DA
90 dB DA
Biphasic Mean
b) Power Spectra
PSD (μV²/Hz)
Frequency (Hz)
c) Normalized MMR vs. DA
NRMSE (%)
7.5 kHz
12.5 kHz
70 dB
90 dB
d) Mean-to-Mean Amplitude
Potential (μV)
7.5 kHz MMR
12.5 kHz MMR
70 dB MMR
90 dB MMR
7.5 kHz DA
12.5 kHz DA
70 dB DA
90 dB DA

11. Legends

Figure 1 Mismatch response computation. a) Classical method. The standard-evoked response is subtracted from the oddball-evoked response. Here the maximum viewing epoch is limited to 1*t*, equal to the stimulus duration plus the inter-stimulus interval. b) Double-epoch method. Here a *standard-standard* pair is subtracted from an *oddball-standard* evoked-response pair. The two second standards are intended to cancel each other out, revealing oddball-induced activity over an extended epoch of 2*t*. Black circles and blue squares represent standard and oddball stimuli, respectively; those selected for respective MMR computations are wrapped in dashed lines.

Figure 2 Grand-average auditory evoked potentials from oddball paradigms. a) 7.5 kHz. b) 12.5 kHz. c) 70 dB. d) 90 dB. The double-epoch subtraction method (Figure 1b) has been applied in each instance to compute the mismatch response (*MMR*) from each respective oddball (*OD*) and standard (*STD*) stimulus-pairs. It may be noted that subsequent to stimulus onset- and offset-evoked activity (<200 ms), a slow biphasic component emerges in frequency and increasing intensity mismatch responses (>200 ms), which is not observed in response to decreasing intensity oddballs. This biphasic component generates positive peak amplitude at approximately 300 to 500 ms, and negative peak amplitude at approximately 600 to 800 ms. The boundary between epochs is demarcated with a vertical dashed line at 550 ms. Shaded regions display sem.

Figure 3 Grand-average auditory evoked potentials from deviant-alone control paradigm stimuli. a) 7.5 kHz. b) 12.5 kHz. c) 70 dB. d) 90 dB. It may be noted that all of the deviant-alone (*DA*) auditory-evoked potentials display a biphasic component with positive peak at 300-500 ms and negative peak at 600-800 ms latency windows. Mismatch response (*MMR*) waveforms are plotted for comparison of this long-latency activity >200 ms post-stimulus-onset. The demarcation line between oddball paradigm epochs is included for reference. It may be noted that both waveforms in a, b, and d appear to follow a similar trajectory of positive to negative potential, albeit with different magnitudes.

Figure 4 Comparison between normalized deviant-alone and mismatch response grand-average waveforms. a) and e) 7.5 kHz. b) and f) 12.5 kHz. c) and g) 70 dB. d) and h) 90 dB. The normalized waveform plots (a-d) are analysed from 200-1000 ms post-stimulus-onset, to remove associated onset and offset activity. These graphs highlight the degree of correspondence between deviant-alone (*DA*) and mismatch response (*MMR*) waveforms across this long-latency window. Fitted polynomials are shown with dotted lines. Scatter plots (e-h) further quantify this relationship, with the concordance correlation coefficient (*CCC*) indicating a high degree of similarity for frequency and increasing intensity stimuli (e, f, and h) and low similarity for decreasing intensity stimuli (g). Straight lines indicate the least-squares linear regression.

Figure 5 Analysis of long-latency auditory-evoked potentials. a) Fitted polynomials. It may be noted that all except the quieter oddball are modelled by a polynomial transitioning from positive to negative between 400 and 600 ms. b) Power spectral density. Measured from mismatch response (MMR) and deviant-alone (DA) waveforms, demonstrating a peak of activity between 2.5 and 5 Hz. c) Normalized root-mean-squared error (NRMSE) between MMR and DA waveforms; *$p = 9.278 \times 10^{-8}$. d) Mean-to-mean amplitude, measured from 300 to 500 ms and 600 to 800 ms post-stimulus-onset; *$p = 6.443 \times 10^{-5}$. Statistics in c) and d) are given from rmANOVA between NRMSE and mean-to-mean amplitude, respectively.